Experimental Investigation of Thermomechanical Effects during Direct Chill and Electromagnetic Casting of Aluminum Alloys

J.-M. DREZET, M. RAPPAZ, B. CARRUPT, and M. PLATA

The deformation and the temperature field within direct chill (DC) and electromagnetic (EM) cast aluminum ingots have been measured *in situ* using a simple experimental setup. The deformation of the cross section of the cold ingots has also been characterized as a function of the casting speed, alloy composition, and inoculation condition. The pull-in of the lateral rolling faces has been found to occur in two sequences for DC cast ingots, whereas that associated with electromagnetic casting (EMC) was continuous. The pull-in was maximum at the center of these faces (about 7 to 9 pct) and strongly depended upon the casting speed. Near the short sides of the ingots, the deformation was only about 2 pct and was nearly independent of the casting parameters and alloy composition. Based upon these measurements, it was concluded that the pull-in of the rolling faces was mainly due to the bending of the ingots induced by the thermal stresses. This conclusion was further supported by a simple two-dimensional thermoelastic model.

I. INTRODUCTION

DURING direct chill casting (DCC)[1] or electromagnetic casting (EMC)[2] of large rectangular rolling sheet ingots of aluminum alloys, the metal deforms in different ways. During the start-up phase, butt curl is critical, especially for EMC, because the meniscus can be destabilized in the electromagnetic field, leading to a premature stop of the casting process. In the steady-state regime of casting, the solidified shell contracts toward the liquid pool, resulting in a nonrectangular shape of the cross section of the ingot. If the alloy is cast in a rectangular mold or inductor, the larger lateral faces of the final ingot are concave (''bone'' shape). To compensate for this effect, the corresponding sides of the mold/inductor are designed with a convex shape, usually with two or three linear segments. Figure 1 shows a schematic top view of a typical mold shape used to produce nearly flat rolling ingots.

At present, the geometry of the mold/inductor is designed mainly by trial-and-error castings for given alloy, casting speed, and ingot size conditions. However, as the sheet ingot dimensional tolerances have become tighter because of scalping and rolling mill demands, the need for casting equipment capable of producing precise ingot geometry has increased accordingly.

A general understanding of the mechanisms involved in the deformation of the metal is therefore highly desirable in order to reduce the time and cost associated with the mold/inductor bow design. In this respect, thermomechanical calculations of the start-up and of the steady-state regime have become an increasingly used tool.[3,4,5] However, because of the many parameters involved in direct chill/electromagnetic (DC/EM) casting, these simulations heavily rely on experimental measurements. Besides, the thermomechanical properties of the cast alloys must be known up to or even above the solidus temperature,[6] and the thermal boundary conditions associated with the lateral water jet have to be estimated through inverse modeling techniques.[7] Once these values are determined, the results of the simulation must be compared with the experiments. Very often, such a comparison is made only on the ''cold'' ingot, and the deformation during the casting process is not measured.

The purpose of the present study is to describe a simple technique for the *in situ* measurement of the deformation and temperature histories during DCC or EMC. In addition to the total deformation of the main body after complete cooling to room temperature, the steady-state temperature profile of the metal during casting, the corresponding shape and depth of the melt pool (''sump''), and the contraction of the solidified shell inside the mold/inductor have been measured. The influence of the casting speed, of the alloy composition, of the grain refinement, and of the air-gap formation during DCC on the deformation of the ingot have been investigated. After analyzing the experimental results, the main mechanisms involved in the deformation of cast ingots are) discussed. These results constitute the basis of a future optimization of the shape of the mold/inductor based on a three-dimensional thermomechanical calculation.

II. LITERATURE SURVEY

The number of articles dealing with the deformation of ingots during semicontinuous casting of aluminum alloys is rather limited. The deformation associated with the starting phase, namely the butt curl and butt swell, has been studied by Yu[8] and Spear and Yu.[8,9] These authors have found that these two distortions can be controlled by a reduction of the heat extracted through the bottom block. Instead of using pulsed water cooling during the start-up phase of the

J.-M. DREZET, Graduate Student, and M. RAPPAZ, Professor, are with the Department des Materiaux, Ecole Polytechnique Federale de Lausanne, MX-G Ecublens, 1015 Lausanne, Switzerland. B. CARRUPT and M. PLATA, Research Engineers, are with the Alusuisse-Lonza Company, CH-3965 Chippis, Switzerland.

Manuscript submitted June 10, 1994.

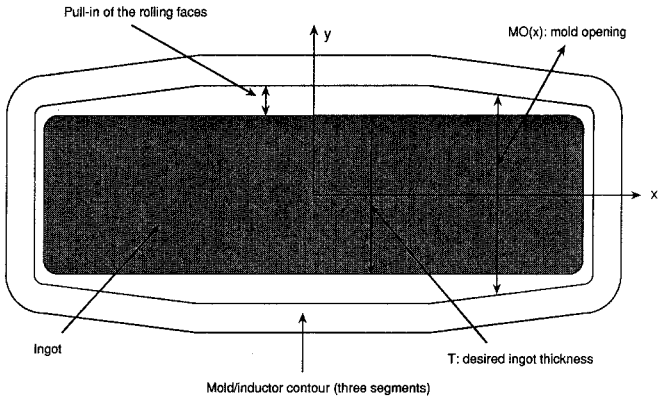

Fig. 1—Schematic top view of the mold/inductor shape required to produce flat rolling sheet ingots.

Table I. Composition (Weight Percent) of the Three Aluminum Alloys

	Fe	Si	Mg	Mn
AA1xxx	0.41	0.14	0.012	0.018
AA3xxx	0.46	0.22	1.14	1.04
AA5xxx	0.24	0.18	2.75	0.27

casting process, they suggested injecting carbon dioxide under high pressure into the ingot cooling water upstream of the mold and covering the bottom block with an insulating pad. Droste and Schneider[10] have studied the effects of the casting velocity and of the cooling water volume on the butt curl and swell of DC-cast aluminum ingots. They showed that the butt curl increased with the casting speed and that very low water volumes and high casting velocities can promote film boiling mechanisms, thus leading to retarded cooling and strongly decreased butt curl.

According to Lawrence,[11] butt swell could be eliminated if a flexible mold was used. Recently, Carrupt and Moulin[12] investigated the effect of the block design on the butt curl formation for both DCC and EMC technologies. They concluded that butt curl is not sensitive to bottom block design when using a reduced cooling technique like carbon dioxide injection or pulsed water.

The deformation of the ingot cross section during the nearly stationary regime of semicontinuous DCC and the mold design required to produce flat sheet ingots have been studied by Weaver.[13,14] Without giving a physically based interpretation of this deformation, this author proposed an empirical model based on casting trials to predict the cross-section changes of DCC ingots. Assuming that the heat extraction was radial (*i.e.*, parabolic shape of the isotherms in the metal under the liquid pool), Weaver derived the relationship

$$MO(x) = K_1 \cdot T + K_2(x) \cdot T^2 \cdot V \qquad [1]$$

where MO is the mold opening as defined in Figure 1, x is the distance to the short sides of the ingot, T is the desired thickness of the ingot, and V is the casting speed. The two alloy-dependent constants, K_1 and K_2, were determined from the experiments. The constant K_1 corresponds to a uniform thermal contraction, and K_2 is a pull-in function that depends on the distance to the short sides of the ingots. Weaver also showed that the mold design required to produce flat ingots changed from a two-straight-lines shape to an almost sinusoidal shape and eventually to a three-straight-lines shape when the aspect ratio of the ingot (width over thickness ratio) was increased.[14]

Since the air-gap formation between the solidifying metal and the mold is directly linked to the pull-in of the rolling faces of the ingot, the heat-transfer mechanisms between metal and mold and the formation of an air gap were also studied intensively, in particular by Ho and Pehlke[15] and by Nishida *et al.*[16] Experimental investigations were conducted by Ozisik *et al.*,[17] whereas Hector[18] developed an interesting theory of growth instability during the solidification of metals in contact with a chilled plate. However, the air-gap formation during the semicontinuous casting of aluminum alloys has not been investigated experimentally.

III. EXPERIMENTAL PROCEDURE

The DCC and EMC trials were carried out at the experimental cast house of Alusuisse with a fully automated casting machine including a control of the metal level in the mold. The nominal ingot cross section was 1860 × 510 mm for the DCC trials and 1800 × 500 mm for the EMC trials; the cast height was typically 3 to 4 m. The casting parameters such as the water cooling flow rate and the) metal distribution bags were kept constant for every combination of alloy and casting speed. A standard 35 deg bottom block, as described by Carrupt and Moulin,[12] was used for all the experiments. During the start phase, a pulsed water cooling technique was employed; *i.e.*, a reduction of 35 pct of the cooling water was applied with a period of 1.3 seconds. A standard water film cooling technique was been employed during the stationary phase with a water flow rate of 800 L/min.

The mold was not optimized specifically for these trial experiments. Its lateral side was made out of three straight lines as shown in Figure 1. The contraction of the ingots cast with this mold was usually too large and nonuniform to fulfill the flatness requirements of an industrial production. Nevertheless, this mold allowed careful measurement of the contraction of the ingot. The inductor used for the EMC trials was designed to produce 500-mm-thickness sheet ingots. The liquid metal was maintained all around the ingot at a constant distance of about 6 mm from a magnetic screen by means of an electromagnetic field produced by a current of 6 kA and 2500 Hz circulating inside the inductor. The inductor and screen were also made out of three straight lines along the rolling faces of the ingot.

Three aluminum alloys were cast with the compositions given in Table I. The grain refiner was the titanium boron aluminum alloy, Al-Ti 5 wt pct-B 2 wt pct.

A. *Deformation Measurement after Cooling*

After complete solidification and cooling of the ingot in the pit, it was reintroduced through the mold/inductor, and the lateral contraction of the ingot was measured at several points of the ingot rolling face and for different heights: in the butt zone, at midheight, and in the upper part (head) of the casting. If the rolling slab is long enough, one can observe mainly three parts: the butt swell which corresponds to the transient starting phase, the central part of the casting

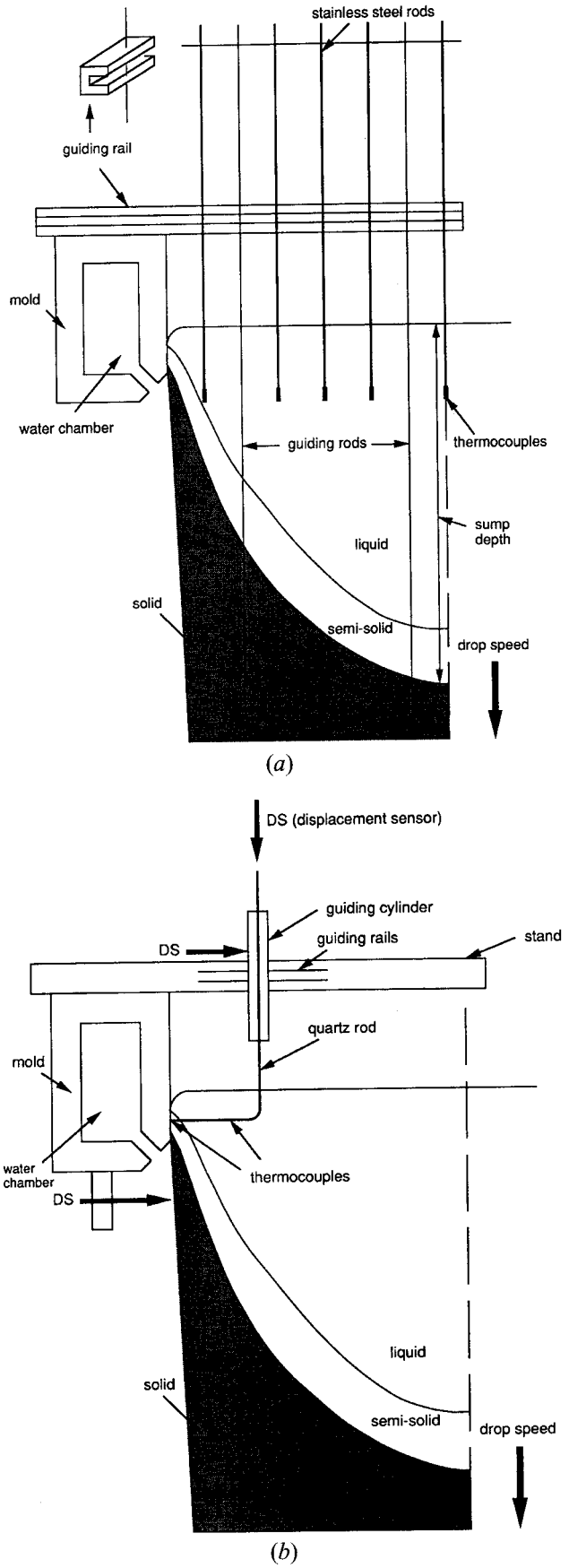

Fig. 2—Experimental setup (*a*) for the measurements of the temperature profile and sump depth and (*b*) for the *in situ* measurement of the casting displacement in the mold/inductor.

which is characterized by a constant contraction and reflects the pseudo steady state, and finally what could be called the head swell. The cast length required to correctly observe these three parts depends on the alloy and on the casting practice, but generally, a length of 3 m is sufficient.[13] In our investigation, the ingots were at least 3-m long to ensure that the measurements at midheight represented the distortion of the ingot in the pseudo steady state.

B. *Sump Depth and Cooling Curves Measurements*

Figure 2(a) shows the experimental setup used to determine the sump depth. This measurement was made at 85 cm from the short side of the casting. A set of five thermocouples attached to the end of stainless steel rods was introduced into the metal during casting after a steady-state regime was reached. The last rod was submerged along the centerline of the ingot, and the first one was near the lateral surface. In order to make sure that the five rods "disappeared" at the constant withdrawal speed in the liquid pool, they were pulled downward by two noninstrumented guiding rods, previously introduced into the metal. During their descent, the rods were guided through a specially designed rail (Figure 2(a)). The thermocouples (type K) were linked to a data logger, and the five temperatures were recorded every 0.1 second. This method allowed the sump depth to be calculated by considering the end of solidification measured by the thermocouple placed at the centerline of the casting. Such measurements also gave the temperature profile in the solid part of the ingot and the shape of the solidification front during the steady-state casting regime.

C. *In Situ Measurement of the Air Gap*

Figure 2(b) shows the experimental setup used to measure the gap distance between the metal and the mold/inductor during the steady state of the process. This setup was located 85 cm from the other short side of the ingot. A quartz rod carrying two thermocouples was introduced into the liquid pool. The rod was free to move downward through a guiding cylinder, and at the same time, it was also free to move along the stand by translation of the cylinder on two guiding rails. The support carriage was able to move with low enough friction to prevent bending of the rod. The quartz rod first dropped into the liquid under its own weight, and) its extremity was then "swallowed" by the mushy zone. From that instant, the quartz rod moved downward at the casting speed of the ingot. When the solidifying metal shell pulled away from the mold surface, the rod followed, and its lateral and vertical displacements were recorded by two sensors. The two thermocouples inserted into the quartz rod measured the temperatures at two locations near the ingot surface (Figure 2(b)). These data permitted more precise assessment of the shape of the mushy zone near the mold wall. In order to test the accuracy of this simple setup, the contraction measured at the exit of the mold/inductor was compared with the value given by a displacement sensor, which was attached to the bottom of the mold/inductor. It is to be noted that the two thermocouple wires were not soldered together since they were directly immersed into the molten aluminum. Thus, the time of entrance of the rod into the liquid pool could be determined accurately from the time of electrical contact.

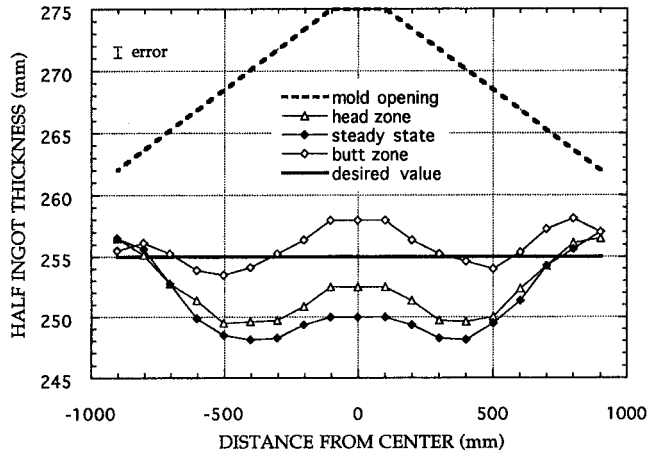

Fig. 3—Contraction of 3xxx DC cast ingot in the starting (butt zone), stationary, and end (head zone) phases and geometry of the mold (casting speed: 70 mm/min, nominal size: 1860 × 510 mm).

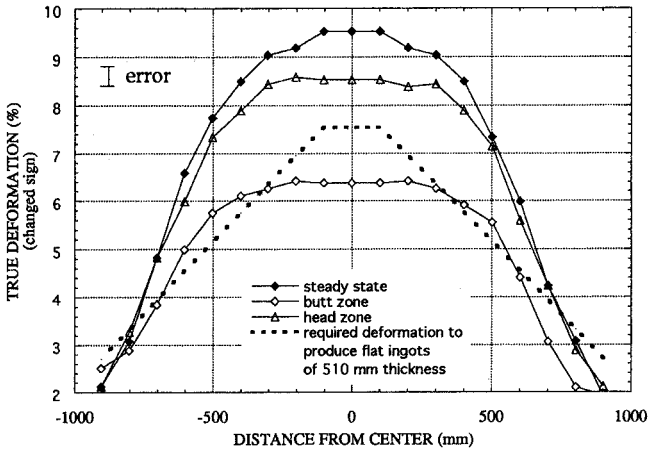

Fig. 4—True deformation (with opposite sign) of the 3xxx ingot cast at 70 mm/min as deduced from Fig. 3.

IV. RESULTS

A. *Deformation of the Cold Ingot*

The three measured cross-section profiles shown in Figure 3 have been obtained for a 3xxx DC ingot cast at 70 mm/min. These profiles have been measured after complete cooling at three different heights of the ingot, and the interior mold shape is also represented for comparison. After a transient stage of about 1 meter, the cross-section shape remains nearly constant: this corresponds to a nearly stationary thermomechanical stage. Near the top of the ingot (head), the section change of the ingot becomes less pronounced, as is the case in the start-up stage. Figure 3 clearly shows that the rolling faces pull-in is important—about 25 mm for the half-ingot thickness at the center of the ingot in the steady-state casting regime. The contraction of the ingot near the two short sides remains nearly constant during the entire casting process. The horizontal line at 255 mm indicates the desired half thickness of a perfectly flat ingot. This value, which is somehow arbitrary, is fixed to a value close to the final thickness of the short sides.

The global ingot deformation is defined as $\log(T/MO)$ where T is the ingot thickness after complete cooling and

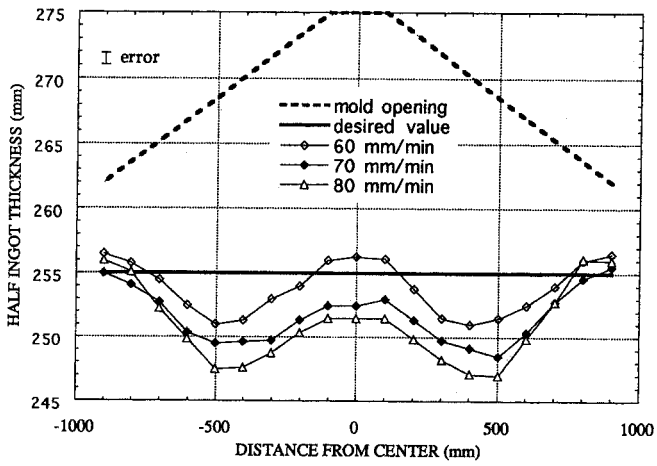

Fig. 5—Influence of the casting speed on the ingot contraction for the alloy 1xxx in the steady-state regime.

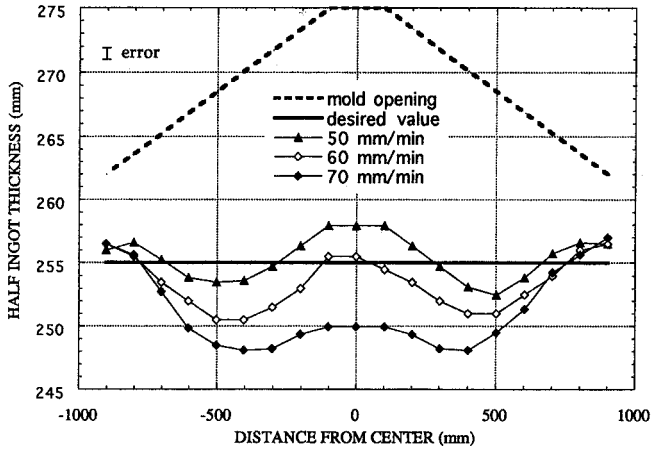

Fig. 6—Influence of the casting speed on the ingot contraction for the alloy 3xxx in the steady-state regime.

MO is the corresponding mold opening. It is shown with the opposite sign in Figure 4. In the steady-state regime of the casting, the metal contraction is about 9.5 pct in the central part of the rolling faces but only about 2.5 pct near the short sides. The required deformation to produce a perfect flat ingot of 510-mm thickness with this mold geometry is also shown for comparison. The contraction near the short sides is slightly less than the desired value, thus leading to a thickness that is slightly larger than expected. At the opposite, the ingot contracts too much in the center when a stationary regime is obtained.

In order to better understand the mechanisms responsible for the deformation of the ingot during the semicontinuous DCC process, the contraction in the steady-state regime of the process was measured for various casting conditions and alloy compositions. The influence of the casting speed on the deformation of the ingot in the stationary regime of casting for the alloys 1xxx and 3xxx is shown in Figure 5 and 6, respectively. For both alloys, it is apparent that the pull-in of the rolling faces center increases with the withdrawal speed, whereas the ends of these faces are almost unaffected by the casting speed.

The influence of the alloy composition and grain refinement on the steady-state deformation is shown in Figure 7,

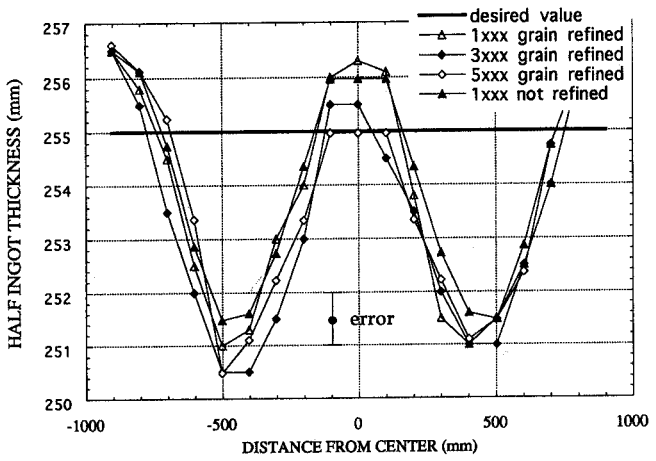

Fig. 7—Influence of the alloy composition and inoculation conditions on the ingot contraction in the steady-state regime (casting speed: 60 mm/min).

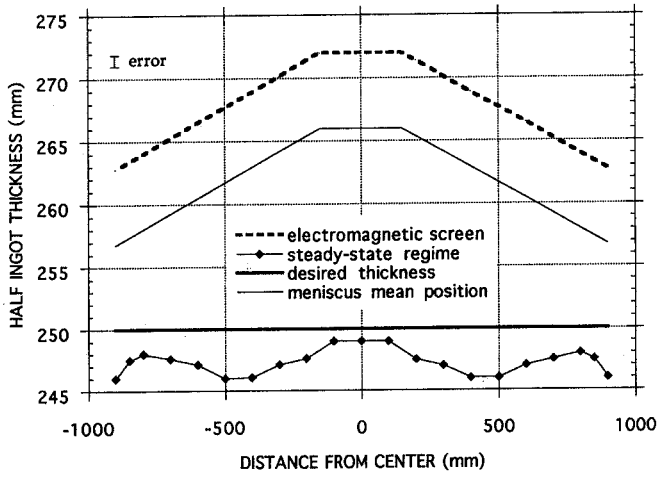

Fig. 8—Contraction of 3xxx EM cast ingot in the stationary phase, geometry of the screen, and estimated position of the meniscus (casting speed: 65 mm/min, nominal size: 1800 × 500 mm).

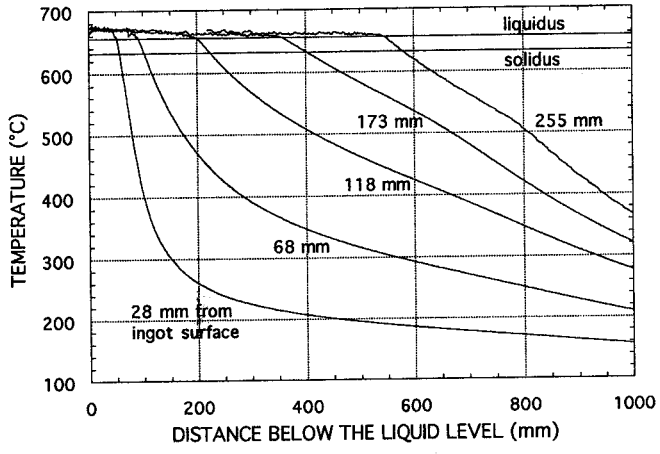

Fig. 9—Measured temperatures during the DCC of a 1xxx alloy ingot cast at 80 mm/min.

for a casting speed of 60 mm/min. The three alloys were grain refined just before casting with 50 ppm of AlTi5B2; the case of the non–grain-refined alloy 1xxx is also shown in this figure. As can be seen, the ingot contraction is not significantly affected by the microstructure; all the measurements fall in a narrow band within the typical error of 1 mm. As for the influence of the casting speed, the alloy composition does not appear to affect the level of contraction near the short sides of the ingot.

The measurement of the EM-cast ingot cross section is shown in Figure 8 for the alloy 3xxx cast at 65 mm/min. The profile of the electromagnetic screen and the estimated position of the liquid meniscus are also plotted. The shape of the liquid free) surface is simply given by subtracting the estimated gap (about 6 mm) from the position of the magnetic screen and neglecting the radius of curvature at the ingot corners.[2] The maximum pull-in in the steady-state regime appears again at the center of the rolling faces and is about 17 mm, which represents a contraction of 7 pct with respect to the estimated free liquid lateral surface. Near the short sides of the ingot, the contraction seems to be larger than in DCC (11 mm in Figure 8). However, because of the radius of curvature of the liquid meniscus at the ingot corners, the effective contraction with respect to the free liquid surface is only about 7 mm. This value is close to that measured for the DC cast ingot shown in Figure 3.

B. *Temperature Profile and Sump Depth*

Figure 9 shows the cooling curves recorded during the DCC of a 1xxx ingot cast at 80 mm/min. The position of the thermocouples from the surface of the ingot is indicated on the figure. Using the withdrawal speed of the ingot, the time scale on the horizontal axis has been converted into the distance from the top surface of the liquid metal. From these measurements, it is apparent that the liquid pool is approximately uniform in temperature (about 665 °C). The temperature at each thermocouple location starts to decrease significantly as soon as the metal begins to solidify.

Figure 10 shows the steady-state temperature profile within the 1xxx ingot during DCC and the sump depth as determined from the five temperature histories of Figure 9. For the alloy 1xxx used in the present investigation, the values of 656 °C and 632 °C for the liquidus and solidus temperatures, respectively, were determined by Gabathuler[19] by means of thermoanalysis (for conditions close to those of the DCC). These values, which are also indicated in Figure 9 by two horizontal lines, were used to evaluate the sump depth. The deep sump depth shown in Figure 10 (580 mm) is due to the high casting speed used for this particular ingot, lower casting speeds resulting in shallower sumps (Table II).

C. *Contraction of the Solidifying Shell*

The recorded temperatures and contraction of the solidifying shell in the mold are shown in Figure 11 for the alloy 5xxx DC cast at 60 mm/min. These data are again represented as a function of the distance below the top liquid surface, as measured by the vertical displacement sensor. They have been measured after a nearly steady-state regime had been reached. These temperatures were recorded at the surface and at 50 mm from the ingot surface. As can be seen, the initial height where the metal and the mold are in good thermal contact is about 30 mm (zone A

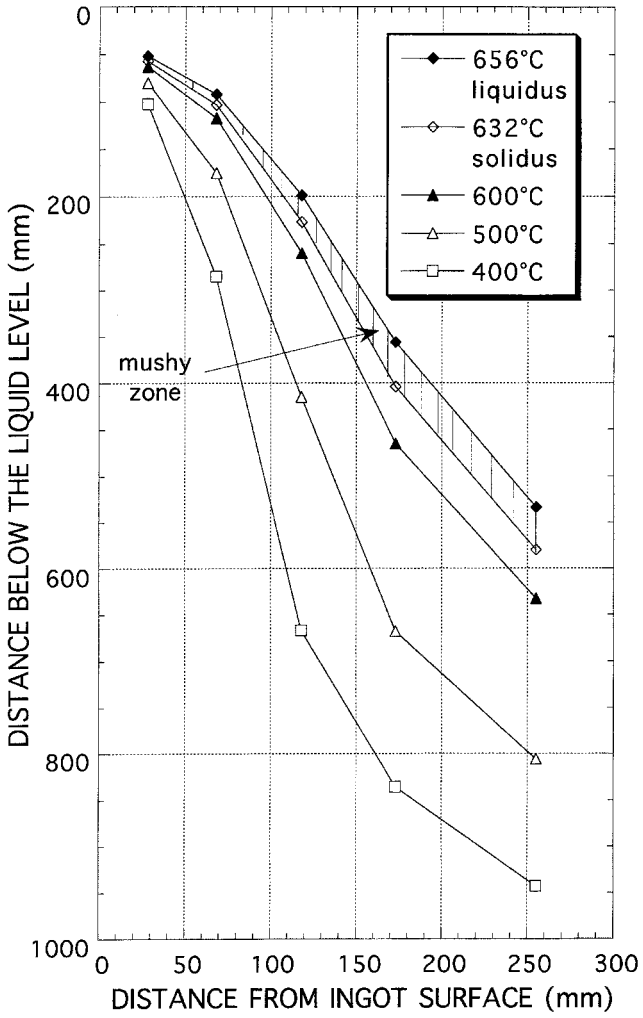

Fig. 10—Temperature profile of the 1xxx alloy ingot during the stationary regime of DCC as deduced from Fig. 9 (casting speed: 80 mm/min).

Table II. Sump Depth for the Alloy 1xxx and Different Casting Speeds (Nominal Size 1860 × 510 mm)

Drop speed	50 mm/min	60 mm/min	80 mm/min
Sump depth	425 mm	480 mm	580 mm

in Figure 11). Then, an air gap forms over a distance of 25 mm (zone B) and remains at a constant clearance of 1.5 mm for the next 20 mm (zone C). After this short plateau, the metal pulls away from the mold at a nearly constant rate (zone D). The displacement of the ingot measured by this moving quartz rod was checked at the exit of the mold with the value recorded by the displacement sensor, which was attached below the mold (Figure 2(b)). The two measurements were in fairly good agreement (typically within 10 pct error). Moreover, the surface temperature at the exit of the mold is too low to allow surface remelting and possible exudation.

The point of impact of the cooling water on the lateral side of the ingot is shown in Figure 11. It almost coincides with the end of the constant air-gap zone. The surface temperature of the ingot just below the cooling water spray is about 200 °C.

As can be seen in Figure 11, the surface temperature of

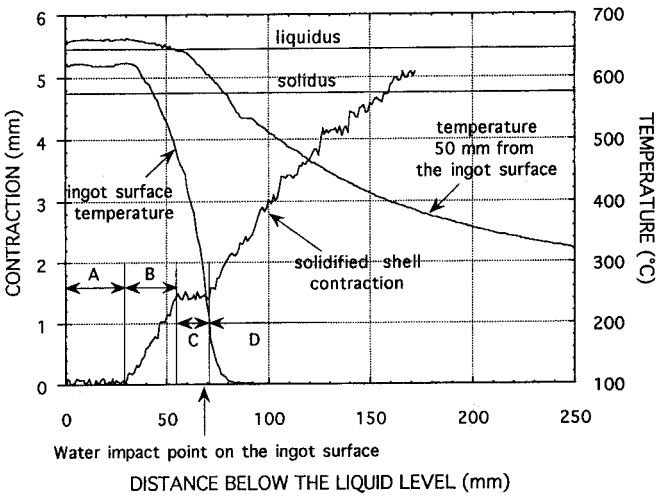

Fig. 11—Measured pull-in and temperatures inside the mold of a 5xxx alloy ingot during DCC (casting speed: 60 mm/min).

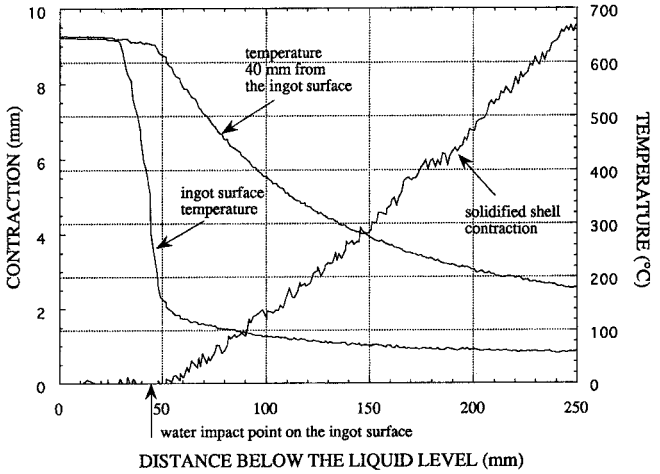

Fig. 12—Measured pull-in and temperatures inside the inductor of a 5xxx alloy ingot during EMC (casting speed: 65 mm/min).

the ingot during contact period A is already below the liquidus of the alloy, whereas, at 50 mm from the surface of the metal, the metal is still totally liquid. Although the temperature measured at the surface of the ingot might be slightly biased by an incomplete wetting of the thermocouple, it increases slightly (about 10 °C) at the onset of the air-gap formation (beginning of zone B in Figure 10) when the heat extraction is decreased. At the temperature of 620 °C measured at the surface of the 5xxx alloy ingot when it pulls away from the mold, the volume fraction of solid is estimated to be about 70 pct according to Gabathuler.[19] Clearly, the metal contraction in the mold occurs when the alloy is still in the semisolid state.

Figure 12 shows the recorded temperatures and displacement of) the solidifying shell during the steady-state EMC regime of an alloy 5xxx cast at 66 mm/min. The displacement plateau observed in DCC (zone C in Figure 11) is no longer present, and the contraction of the shell just below the point of impact of the cooling water occurs at a nearly constant rate. At 250 mm below the top liquid surface, the

rolling face pull-in is almost 10 mm. The two temperatures within the EMC ingot were recorded at the lateral surface and at 40 mm from the surface. The surface temperature at the point of impact of the water cooling is about 200 °C, as was already the case for the DCC process. Above this point, the temperature within the liquid near the surface is much more uniform than in DCC due to, first, the absence of a direct contact with a mold and, second, the strong convection induced by the electromagnetic field.[20]

V. DISCUSSION

Weaver[13,14] has explained the ingot deformation occurring during semicontinuous casting in terms of the extension of the liquid pool and of the shape of the solid shell. This model is based on the hypothesis that the heat extraction is uniform and horizontal. As seen in Figure 10, this is clearly not the case. Moreover, the model of Weaver requires numerous casting trials for the estimation of the alloy-dependent constants K_1 and K_2 (Eq. [1]). The present experimental investigation, in particular the *in situ* measurements of the temperature field and of the surface pull-in of the rolling faces, allows clearer assessment of the main mechanisms leading to the nonuniform contraction of the ingot during DC/EM casting.

A. *Contraction of the Metal during Solidification*

During solidification of a metal, there are essentially two contributions to the ingot contraction, the first one being associated with the phase change (about 6.5 pct in volume for aluminum[21]) and the second contribution arising from the solid state thermal contraction during subsequent cooling (about 1.5 pct). During the liquid-to-solid phase transformation, there is a constant liquid feeding within the mushy zone to compensate for the density variation. For an aluminum-4.5 wt pct copper alloy, it has been shown that the associated pressure drop within the liquid is not more than one-tenth of the atmospheric pressure when no microporosity forms.[22] For alloys having an even larger solidification interval (*e.g.*, Al-Mg), feeding is more difficult, and as a result, microporosity may develop more easily. Micrographs of the as-cast ingots revealed almost no microporosity. In any case, the pressure drop of the liquid within the mushy zone induced by the density change between the liquid and solid phases is certainly too low to explain the section change of the cast ingots.* Considering Figure 11, for example, it is seen that the initial pull-in (up to the plateau labeled "C") only represents 1.5 mm (*i.e.*, 0.6 pct) of contraction. At the end of this plateau (*i.e.*, 70 mm below the top liquid surface), the surface is totally solid, and the solidus line is already 30 to 40 mm in the interior of the ingot (Figure 10). Thus, the solid skin of the ingot is already well developed and cannot be deformed by the pressure drop of the liquid within the mushy zone.

The 9.5 pct pull-in measured at the ingot center during DCC or the 7 pct pull-in measured during EMC after complete cooling is therefore a consequence of the deformation of the solid ingot. Although thermal contraction is only 1.5 pct for a uniform temperature specimen, the *cumulated deformation* and associated *bending* during continuous casting can explain the large pull-in of the rolling faces. Such a mechanism, which is supported by the transient deformation state near the bottom of the ingot (Figure 3), is detailed in Section B.

B. *Inward Pull-In of the Rolling Faces*

During cooling, the metal experiences a high nonuniform thermal gradient (Figure 10) that gives rise to differential thermal contraction and high stresses that can be partially relieved by creep. During DCC, the alloy undergoes two different coolings, the first one when it is in direct contact with the mold and the second one under the cooling water spray. This leads to the appearance of a thin solid shell in between the two cooling zones and nearly parallel to the mold. This thin shell contracts under the high) local thermal gradient (Figure 11), the metallostatic pressure being too small to withstand the displacement of the solidified shell. On the contrary, during EMC, the metal experiences only one cooling, the water spray, and the deformation is continuous (Figure 12). However, at about 100 mm below the top liquid surface, the contraction is about the same in both processes (2.5 mm or 1 pct deformation). At this height, the solid skin is already well developed and extends beyond the second thermocouple attached to the quartz rod; *i.e.*, the surface skin is at least 40- to 50-mm thick in both DC and EM casting. Such a skin continues to thicken and deform during further cooling of the casting.

The calculation of butt curl and swell during the start-up phase of DC casting has already been performed by several authors.[3,4,5] A similar investigation is being carried out for the pull-in of the rolling faces. Such calculations require a precise knowledge of the boundary conditions and of the thermomechanical properties of the alloy. Furthermore, they must be performed for an evolutive domain. Although the results of such calculations are not yet available, a simpler situation can be considered for the understanding of the deformation of DC or EM cast ingots. The domain shown in Figure 13(a) is assumed to represent a portion of the midplane section of a DC casting in the steady-state regime, the left and right boundaries coinciding with the plane of symmetry of the ingot and with the rolling face, respectively. This domain extends from the solidus surface, taken as a straight line, to a parallel line below where the temperature is equal to room temperature. The thermal gradient in the piece is supposed to be uniform, and therefore, the lower boundary is taken to be parallel to the upper boundary for the sake of simplicity. It should be noted that taking a horizontal boundary for the room-temperature isotherm does not change significantly the contraction of the top right corner (this has been verified by a numerical calculation). The thickness of the parallelogram is half that of the ingot (275 mm), and its length is typically that needed to establish a stationary regime (taken as 1.2 m in the present case). The angle of the parallelogram, θ, is calculated from the sump depth (Table II). The model is thermoelastic; *i.e.*, the total deformation is the superposition of an elastic and a thermal component, and the thermophysical properties of the alloy are temperature independent (Table III).

*In the case of no microporosity formation and incomplete liquid feeding, the maximum solid deformation associated with the shrinkage in the mushy zone would be lower than the maximum level of microporosity, which could be expected to be in such alloys about 1 pct in volume fraction and represent a maximum linear contraction of about 0.3 pct.

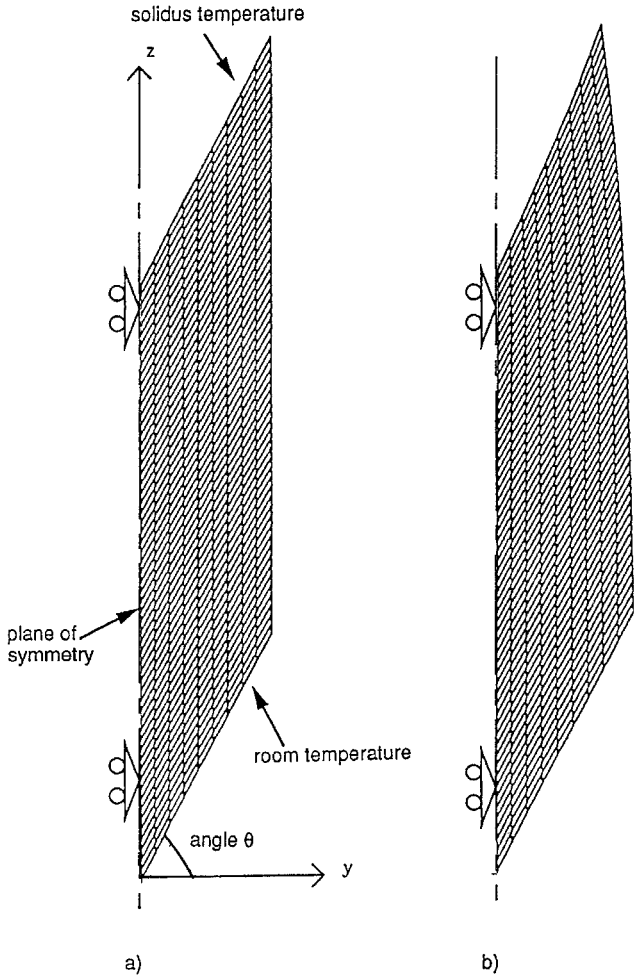

Fig. 13—Two-dimensional longitudinal section of the continuously cast ingot used in (*a*) the thermoelastic model and (*b*) the deformed domain after complete cooling. The displacements have been magnified by a factor of 5.

Table III. Thermophysical Parameters and Thermal Field Used in the Simplified Model for a Cast Length of 1.2 m

Solidus temperature	650 °C
Young's modulus	70 GPa
Poisson's ratio	0.35
Linear expansion coefficient	30.10^{-6}/K
Thermal gradient:	
y component	$-525 \cdot tg\theta$ K/m
z component	525 K/m

The deformation of this volume when it cools down to a uniform temperature has been calculated with ABAQUS,*

*ABAQUS is a trademark of Hibbitt, Karlsson, and Sorensen, Inc., Providence, RI.

under the assumption of plane strains. The left boundary is assumed to remain vertical during cooling for symmetry reasons.** The deformed domain is shown in Figure 13(b)

**If the whole boundary of the domain is free of any constraint, then a linear temperature field does not create stresses: the differential thermal contractions are accommodated through a rotation of the domain.

with an amplification factor of 5 for the displacements. The

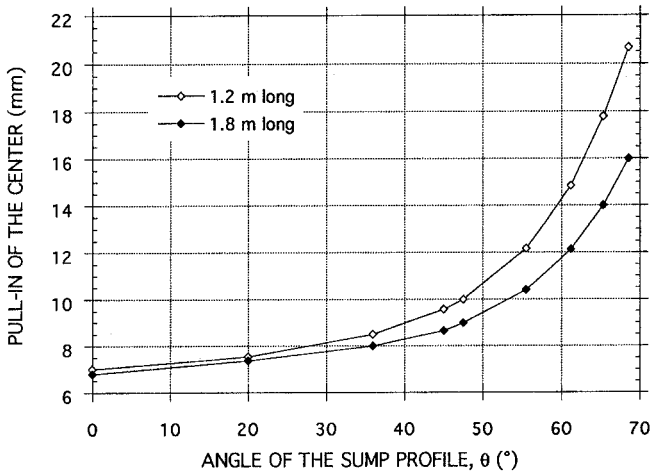

Fig. 14—Pull-in of the center of the rolling faces after complete cooling as a function of the average angle of the sump profile θ. The two sets of points correspond to two different lengths (and thus thermal gradients) of the domain.

deformation of the top corner of the ingot is about 15 mm (pull-in of 5.5 pct). This value, which is much larger than the overall thermal contraction of 1.5 pct, is due to the shearing associated with a nonsymmetric temperature repartition[23] and with the inclination of the parallelogram (θ = 61.2 deg in the case of AA1xxx cast at 60 mm/min). Although rudimentary, this simple model explains the importance of the pull-in at the midrolling faces of the ingot: it is mainly due to the bending associated with the thermal stresses that develop upon cooling of the ingot. The model also gives the correct dependence of the pull-in upon an increase of the sump depth, *i.e.*, an increase of the angle θ, or, equivalently, of the casting speed (Table II). Figure 14 shows the pull-in of the top right corner of the domain as a function of the angle θ, all the other conditions remaining the same. As can be seen, the deformation increases with θ, especially above 45 deg, thus qualitatively reproducing the trend observed in Figures 5 and 6. The two sets of points correspond to two different heights of the domain. Surprisingly, the pull-in of the top right corner decreases with increasing length of the domain: this is due to the thermal gradient, which also decreases with the length.

According to this simple model, the dependence of the rolling faces pull-in upon the composition of the alloy (Figure 7) is believed to be associated mainly with variations of the sump depth (through a modified thermal conductivity) and mechanical properties, rather than with a modification of the solidification interval of the) alloy. The different pull-in measured for the DC and EM castings is therefore most probably due to the difference in thermal gradients induced by the respective water cooling. Indeed, for the same casting speed, the sump of a DC cast ingot is deeper than that of an EM cast ingot as a result of the two cooling sequences; consequently, according to the model, the angle θ corresponding to the DC casting is higher, thus leading to larger pull-in as shown in Figure 14.

During the start-up phase, the initial pull-in of the ingot is found to be lower than during the steady-state regime (Figure 3). This is also partially explained by the simple model shown in Figure 13. The bottom part of the ingot starts to deform when the cooling water impinges on the

lateral surface.[3,4,5] The associated bending tends to lift the ingot from the bottom block, but the lateral displacement is not important at that time (of the order of the thermal contraction). Then this part is too thick and too cold to deform during further solidification of the ingot, as shown in Figure 13. The transient deformation measured near the top of the ingot (Figure 3) is associated with a decreased length of the casting over which possible bending can occur. However, the trend seen in Figure 14 for the effect of the length of the calculation domain is no longer valid since shrinkage associated with the absence of liquid and nonsteady thermal effects may also modify the pull-in of the rolling faces near the head of the ingot.

C. *Three-Dimensional Aspects: Edge Reinforcement*

As shown by the experiments, the contraction of the edges in the y direction of the casting (Figure 1) is much smaller (about 2.5 pct) and almost unaffected by the cast length (Figure 3), by the casting speed (Figures 5 and 6), and by the alloy composition (Figure 7). This effect is also qualitatively reproduced by the simple model presented before. Near the short sides of the ingot, the sump may have about the same shape as along the rolling faces, but it is now turned 90 deg with respect to the situation considered before for the center of the rolling faces. Accordingly, the pull-in of the short sides along the y direction (Figure 1) corresponds to the situation for which $\theta = 0$. As can be seen in Figure 14, the deformation in this case is only 7 mm (pull-in of 2.5 pct) and agrees fairly well with the measurements. In other words, the pull-in of the short sides of the ingots is close to the contraction of an ingot that is continuously cast at very low speed, *i.e.*, close to the thermal shrinkage seen in a mold-cast ingot cooled from the bottom.

The nonuniform deformation of the ingot in between the short sides and the center of the rolling faces is therefore qualitatively understood, but a quantitative analysis would have to account for three-dimensional and viscoelastic effects. The design of the mold/inductor at the center and edges of the rolling faces can be calculated so as to have the same final dimension, considering, for example, the simple arguments presented here. However, the use of three straight segments is oversimplistic if truly flat ingots are to be produced. Such design indeed can diminish the variation of the ingot thickness around an average value (*i.e.*, can decrease the concavity of the final bone-shape ingot), but it clearly undercorrects the pull-in along the inclined segments (Figure 3, for example).

VI. CONCLUSION

The ingot deformation during DC/EM casting has been measured *in situ* in order to elucidate the mechanisms responsible for the large and nonuniform contraction of the ingot cross section. It appears that the air-gap formation in DCC is only 0.5 pct near the center of the rolling faces, whereas the total deformation after complete cooling of the ingot is about 9 pct. This rules out any influence of the solidification shrinkage. Thus, it is concluded that the pull-in of the faces is due only to the thermal stresses that develop upon cooling of the ingot. Although linear thermal contraction is only 1.5 pct in aluminum alloys, the horizontal component of the temperature gradient introduces a bending of the ingot. A simple thermoelastic model already predicts a pull-in of at least 5 to 6 pct at the center of the rolling faces in a steady-state regime. Although creep certainly needs to be taken into account, this model also gives a fairly accurate) description of the much smaller pull-in measured near the short sides of the ingot. The effect of the casting speed on the cross-section contraction is also qualitatively reproduced by the model.

The prediction of the ingot deformation for a given mold/inductor bow would allow optimization of the design of a mold/inductor capable of producing flat ingots. This problem requires use of a three-dimensional model that adequately takes into account the shape of the sump profile, the edge reinforcement, and the viscoelastic behavior of the alloy.

ACKNOWLEDGMENT

The financial support of Alusuisse Lonza Services Ltd., Chippis, and of the Commission pour l'Encouragement de la Recherche Scientifique (CERS), Bern, under Grant No. 2496.1, is gratefully acknowledged.

REFERENCES

1. E.F. Emley: *Int. Met. Rev.*, 1976, June, pp. 75-115.
2. Y. Kraĥenbuĥl, R. Von Kaenel, B. Carrupt, and J.C. Weber: *Light Met.*, TMS, AIME, Warrendale, PA, 1990, p. 893.
3. H. Fjaer and A. Mo: *Metall. Trans. B*, 1990, vol. 21B, pp. 1049-61.
4. S. Mariaux, M. Rappaz, Y. Kraĥenbuĥl, and M. Plata: *Light Met.*, TMS, AIME, Warrendale, PA, 1992, p. 175.
5. B. Hannart, F. Cialti, and R.V. Schalkwijk: *Light Met.*, TMS, AIME, Warrendale, PA, 1994, p. 879.
6. J.M. Drezet and G. Eggeler: *Scripta Metall. Mater.*, 1994, vol. 31, p. 757.
7. J.V. Beck, B. Blackwell, and J.R. St Clair: *Inverse Heat Conduction*, Wiley Interscience, New York, NY, 1985.
8. Ho Yu: *Light Met.*, TMS, AIME, Warrendale, PA, 1980, p. 613.
9. R.E. Spear and H. Yu: *Aluminium*, Communication from Alcoa Laboratories, Alcoa Center, PA, 1984, p. 440.
10. W. Droste and W. Schneider: *Light Met.*, TMS, AIME, Warrendale, PA, 1991, p. 945.
11. R.R. Lawrence: *Cross-Section Shape Control of D.C. Sheet Ingot Using a Flexible Mold, Light Met.*, TMS-AIME, Warrendale, PA, 1976, p. 457.
12. B. Carrupt and C. Moulin: *Effects of Casting Technology and Bottom Block Design on Butt Curl Formation with Rolling Slabs*, 8th International Sheet and Plate Conference, Louisville, KY, Oct. 5–8, 1993.
13. C.H. Weaver: *An Empirical Model to Explain Cross-Section Changes of D.C. Sheet Ingot during Casting, Light Met.*, TMS-AIME, Warrendale, PA, 1976, p. 441.
14. C.H. Weaver: *Light Met.*, 1991, p. 953.
15. K. Ho and R. Pehlke: *Metall. Trans. B*, 1985, vol. 16B, pp. 585-94.
16. Y. Nishida, W. Droste, and S. Engler: *Metall. Trans. B*, 1986, vol. 17B, 833-44.
17. M.N. Ozisik, H. Orland, L.G. Hector, J.R. Anyalebechi, and P.N. Anyalebechi: *J. Mater. Proc. Manufact. Sci.*, 1992, vol. 1, p. 213.
18. L.G. Hector: *Mech. Res. Commun.*, 1991, vol. 18, p. 51.
19. J.P. Gabathuler: *Thermoanalyse*, Alusuisse internal technical report, June 1985.
20. O. Besson, J. Bourgeois, P.A. Chevalier, J. Rappaz, and R. Touzani: *J. Comput. Phys.*, 1991, vol. 92 (2), p. 482.
21. L.F. Mondolfo: *Aluminum Alloys: Structure and Properties*, Butterworths, Boston, MA, 1976.
22. J. Ampuero, A.F.A. Hoadley, and M. Rappaz: in *Modeling of Casting, Welding and Advanced Solidification Processes 5*, M. Rappaz, M.R. Ozgu, and K.W. Mahin, eds., TMS, 1991, p. 449.
23. S.P. Timoshenko and J.N. Goodier: *Theory of Elasticity*, 3rd ed., McGraw-Hill Kogakusha Ltd., Singapore.